



Geophysical Research Letters

Supporting Information for

Hydrologic Sensitivities of Terrestrial Evaporation and Moisture Drainage in a Warmer Climate

Daniel J. Short Gianotti¹, Ruzbeh Akbar¹, Andrew F. Feldman¹, Guido D. Salvucci², Dara Entekhabi¹

¹Parsons Laboratory, Department of Civil and Environmental Engineering, Massachusetts Institute of Technology

²Department of Earth and Environment, Boston University

Corresponding Author: Daniel J. Short Gianotti (gianotti@mit.edu)

Contents of this file

Changing precipitation extremes (P_{X90})
Figures S1 to S9

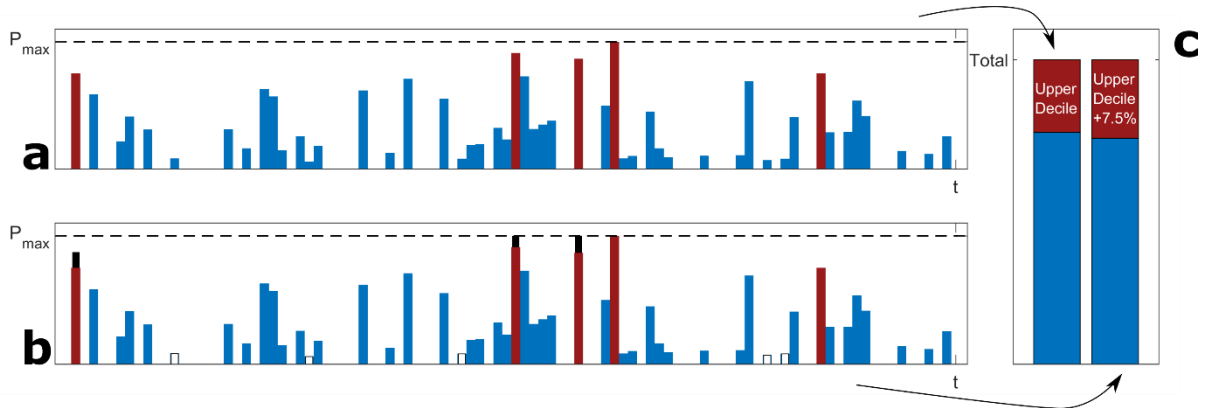
Introduction

This document provides supplementary information for the GRL article, “Hydrologic Sensitivities of Terrestrial Evaporation and Moisture Drainage in a Warmer Climate,” specifically Figures S1 to S8. Figures were created following the methods outlined in the main text (following the methods of Akbar et al. (2019) for flux estimation and soil moisture states). All other information is contained within the main text.

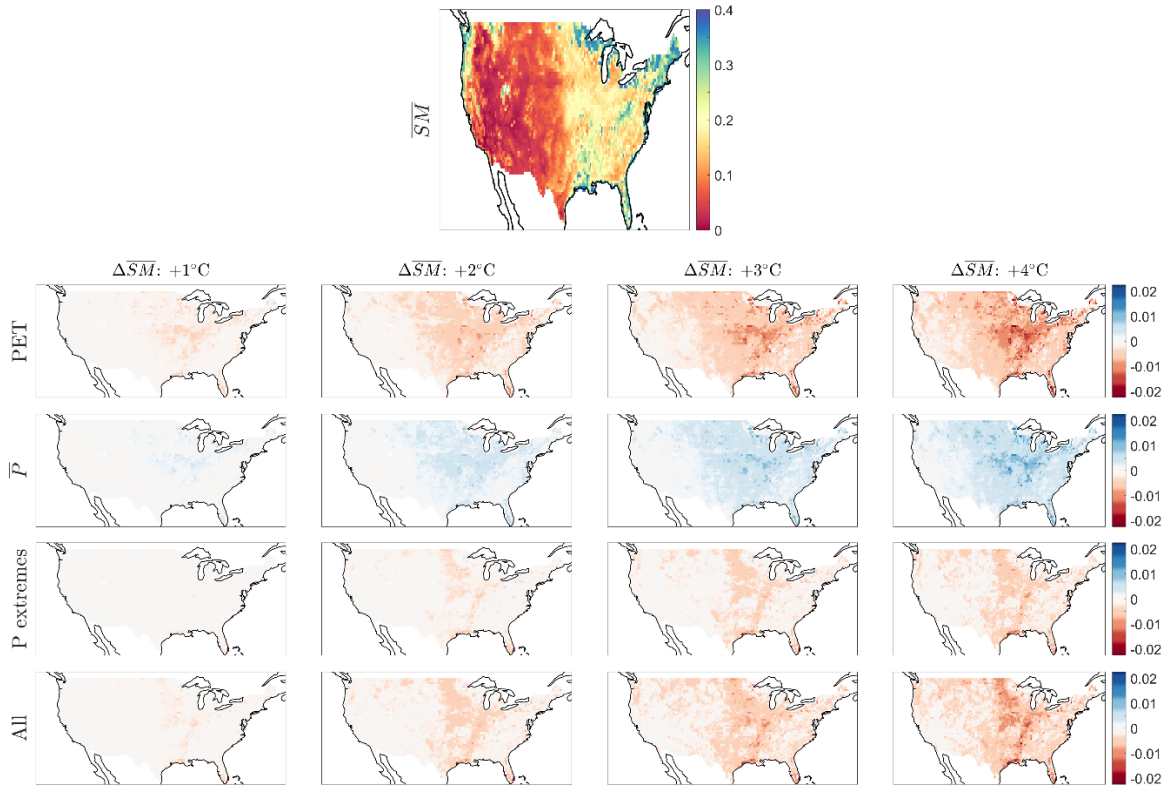
Changing precipitation extremes (P_{X90})

For our precipitation extremes experiment, precipitation is re-allocated from the dry tail of the precipitation distribution to the wet tail. This is performed by first calculating the total precipitation in the upper decile of the precipitation intensity distribution (ignoring days with no rainfall), referred to as P_{X90} . This value is multiplied by a scaling factor $1 + m \cdot w$,

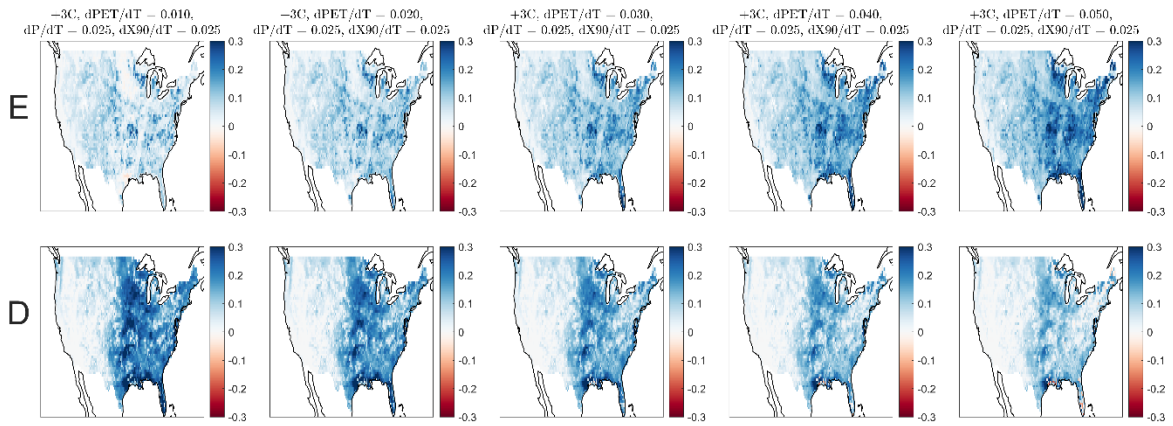
using $w = 0.025$ and $m = \{1,2,3,4\}$ by increasing the intensity of the 2nd wettest day until it is equal to the wettest day, then the 3rd wettest until it equals the wettest, etc., until P_{X90} has increased by the desired amount $m \cdot w \cdot P_{X90}$. An equal amount is removed from the dry tail of the distribution by setting the driest day with some rain to have no rainfall, then the 2nd driest, etc., until the $m \cdot w \cdot P_{X90}$ precipitation has been reallocated from the dry tail to the wet tail. This leaves the mean precipitation and event timing unchanged, but increases the number of dry days. See Supplementary Figure 1.



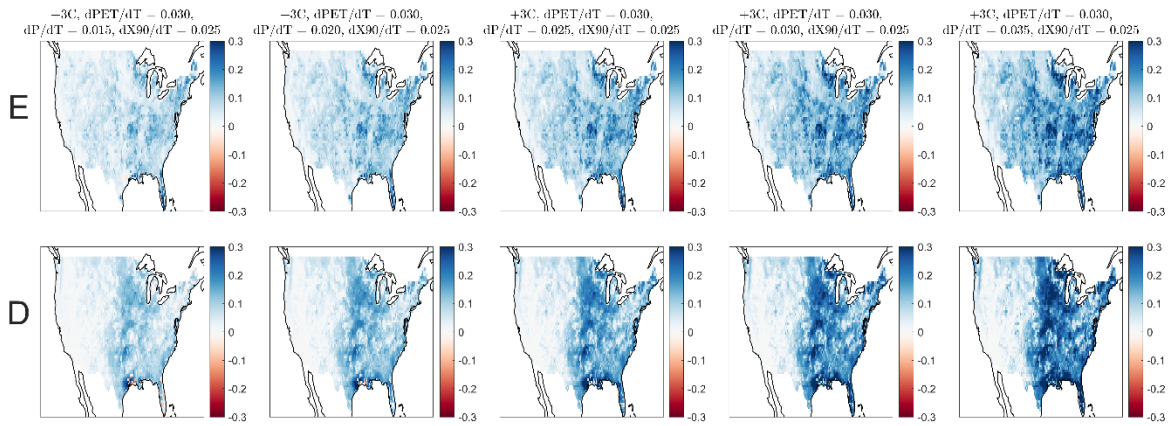
Supplementary Figure 1: Changes to precipitation extremes. To increase precipitation extremes without changing mean or maximum observed precipitation, we move precipitation from low precipitation days to high precipitation days. a) A simulated time series of precipitation, with the upper decile (10% wettest) days shown in red. Of the 50 days with measured precipitation, the five heaviest (red) days contribute a sizeable portion of seasonal total rainfall (shown in the left bar chart of (c)). b) Extremes (P_{X90}) increased by 7.5%. To increase the precipitation in the upper decile of days by 7.5% (as seen in the right bar of (c)), precipitation equal to 7.5% of the red area in (a) is taken from the driest days, shown in white. This precipitation is added to the 2nd wettest day (added precipitation shown as black bar) until precipitation on that day equals that of the heaviest observed day, P_{max} . Precipitation from the dry days is then added to the 3rd wettest day, and the 4th, until all of the additional 7.5% of the upper decile precipitation has been re-allocated. The seasonal total is unaffected, as is the maximum precipitation. Some of the driest days now have zero precipitation (white bars), and three of the wettest days are somewhat wetter. All other days' precipitation is unchanged.



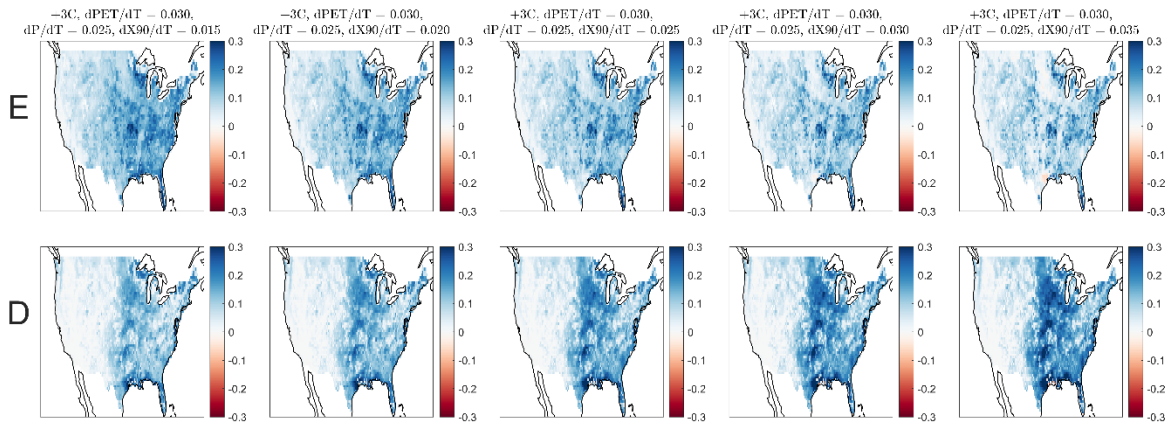
Supplementary Figure 2: Changes in mean soil moisture. Mean surface soil moisture from data-assimilated brightness temperatures from SMAP for May-September 2015-2017 in mm^3/mm^3 (top panel). The second row shows changes in surface soil moisture (in mm^3/mm^3) relative to the top panel due to just E_o changes (as in Main Text Figure 2b) for 1-4°C changes in surface air temperature (3-12% changes in local PET). The surface dries in all locations, as expected. The third row shows changes in surface soil moisture (in mm^3/mm^3) relative to the top panel due to just changes in mean precipitation (as in Main Text Figure 2c) for 1-4°C changes in surface air temperature (2.5-10% changes in local mean precipitation); the surface wets in all locations. The fourth row shows changes in surface soil moisture (in mm^3/mm^3) relative to the top panel due to just changes in extreme precipitation (as in Main Text Figure 2d) for 1-4°C changes in surface air temperature (2.5-10% changes in local mean precipitation); the surface dries in all locations. The fifth row shows changes in surface soil moisture (in mm^3/mm^3) relative to the top panel due to synchronous changes in all of PET, mean precipitation, and extreme precipitation (as in Main Text Figure 2e) for 1-4°C changes in surface air temperature; the surface dries in all locations.



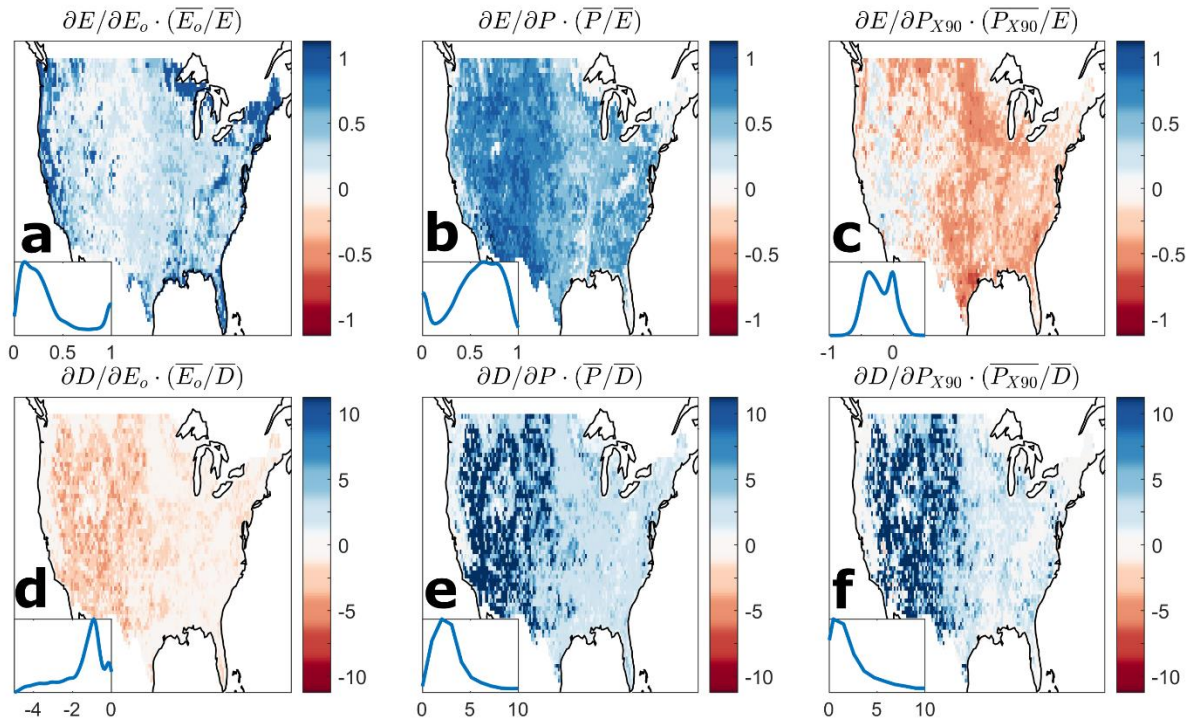
Supplementary Figure 3: Sensitivity of results to $d\text{PET}/dT$. Changes in evaporation (E) and drainage (D) from the present day observations (Main Text Figure 2a) for a $+3^\circ\text{C}$ scenario (compare to 3rd column, Main Text Figure 2b-d), using differing values for the sensitivity of PET to temperature, from $1\%/^\circ\text{C}$ to $5\%/^\circ\text{C}$. Sensitivities for mean and extreme precipitation stay the same as in Main Text Figure 2.



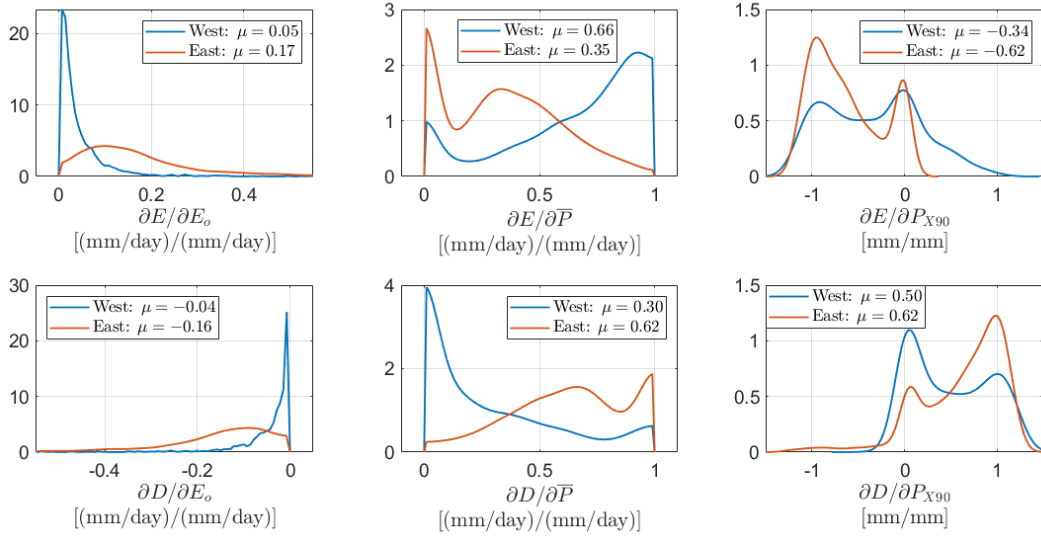
Supplementary Figure 4: Sensitivity of results to dP/dT . Changes in evaporation (E) and drainage (D) from the present day observations (Main Text Figure 2a) for a $+3^\circ\text{C}$ scenario (compare to 3rd column, Main Text Figure 2b-d), using differing values for the sensitivity of mean precipitation to temperature, from $1.5\%/^\circ\text{C}$ to $3.5\%/^\circ\text{C}$. Sensitivities for PET and extreme precipitation stay the same as in Main Text Figure 2.



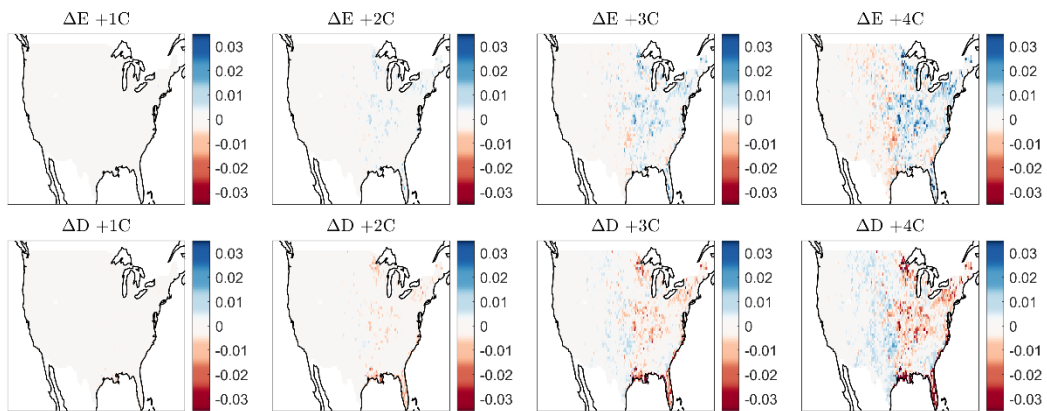
Supplementary Figure 5: Sensitivity of results to dX_{90}/dT . Changes in evaporation (E) and drainage (D) from the present day observations (Main Text Figure 2a) for a $+3^{\circ}\text{C}$ scenario (compare to 3rd column, Main Text Figure 2b-d), using differing values for the sensitivity of extreme precipitation to temperature, from $1.5\%/^{\circ}\text{C}$ to $3.5\%/^{\circ}\text{C}$. Sensitivities for PET and extreme precipitation stay the same as in Main Text Figure 2.



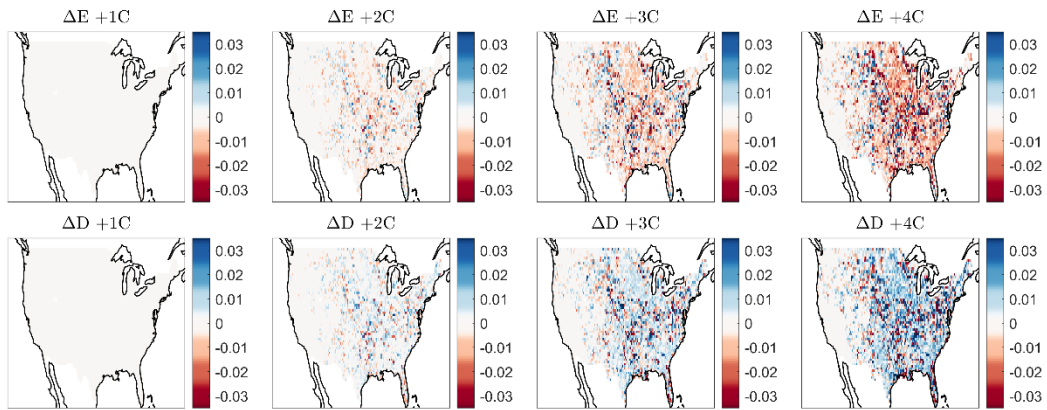
Supplementary Figure 6: Elasticities. a-c) Elasticities of evaporation with E_o , \bar{P} , and P_{X90} respectively. A 1% increase in E_o corresponds to up to a 4% increase in E in the darkest blue areas. A 1% increase in mean P contributes up to a roughly equal percent increase in E. A 1% increase heavy (top decile) precipitation corresponds to roughly a 0.5% decrease in E across the Central Plains. Insets show probability density of mapped values. d-f) Elasticities of drainage, as in c-e. Evaporation is more sensitive to relative changes in \bar{P} than E_o in 74% of pixels; drainage is more sensitive to relative changes in \bar{P} than E_o in 99% of pixels (in an absolute value sense).



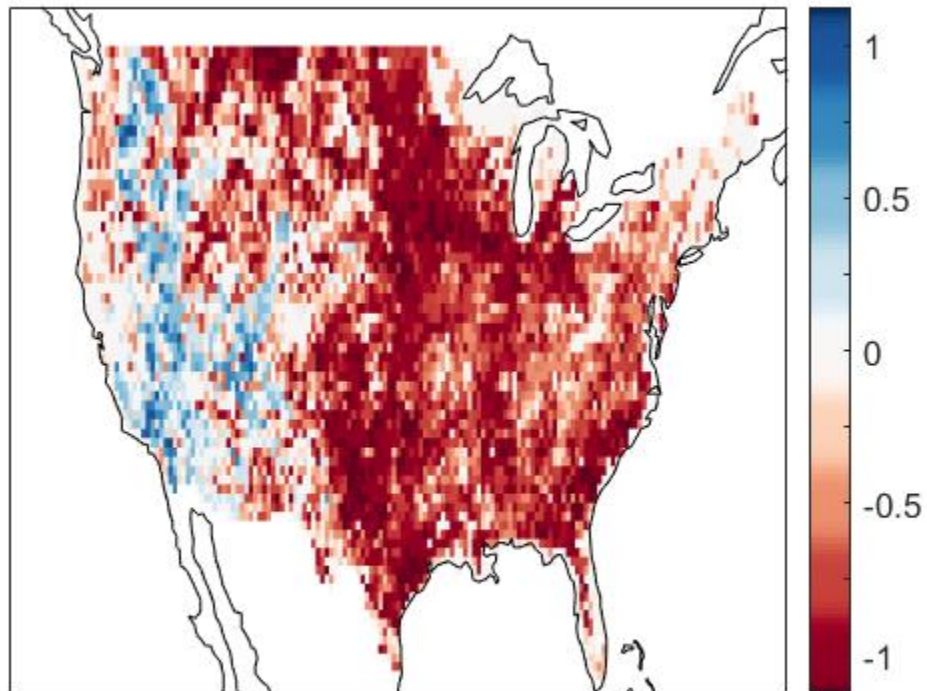
Supplementary Figure 7: Probability densities for East/West ConUS. Top row, left: Probability density functions (PDFs) of the partial derivative of evaporation (E) with respect to changes in potential evaporation ($\partial E / \partial E_o$). Blue shows the distribution for locations west of 98°W , red shows the distribution for locations east of 98°W . The more energy-limited Eastern ConUS shows larger changes in E for a given change in E_o , with an average of 0.17 mm/day increase in E for every 1 mm/day increase in E_o (roughly 3.5 times larger effect than in the Western ConUS). Top row, middle: PDFs of the partial derivative of evaporation with respect to changes in mean precipitation ($\partial E / \partial \bar{P}$). Increasing moisture supply (as opposed to E_o demand) shows greater evaporative increases in the more arid West; values fall strictly between 0 (no change; fully energy limited or very large hydraulic conductivity) and 1 (all additional water goes to evaporation; fully water limited). Mean Top row, right: PDFs of the partial derivative of seasonal total evaporation with respect to changes in heavy precipitation ($\partial E / \partial P_{X90}$). Heavy precipitation in the upper decile of the precipitation distribution is increased by ΔP_{X90} mm (max and mean precipitation are unchanged) at the expense of an equivalent precipitation from the light tail, so that $\partial E / \partial P_{X90}$ is the change in E (mm over the season) for every 1 mm of precipitation added to the upper decile of the P distribution. Increasing extremes reduces evaporation more in the East (by further increasing drainage). Bottom row: Same as top row, but for drainage (D) instead of E.



Supplementary Figure 8: Linear additivity of the separate PET, mean P, and P extremes effects. Each map shows the difference in E or D when subtracting the individual perturbation effects (Main Text Figure 2b-d) from the combined model including all processes (Figure 2e).



Supplementary Figure 9: Linearity of temperature scaling. Each map shows the difference when subtracting the scaled changes in E or D using ΔT multiplied by the $+1^\circ\text{C}$ ΔE or ΔD map from the model representing the scaled sensitivity perturbation directly (i.e., subtracting 4 times column 1 from column 4 in Main Text Figure 2e).



Supplementary Figure 10: $\partial E / \partial P_{\chi 90}$. Blue regions in the arid West show areas where increased extremes increase evaporation, and red regions see decreased evaporation. Values in mm of seasonal evaporation per mm of precipitation moved from the driest days to the upper decile. Regions with increased evaporation are where changes in extremes push soil moisture into somewhat dry conditions (“Stage II” evaporation) where $E(\theta) \gg D(\theta)$ from *very* dry conditions (“Stage III” evaporation) where $E(\theta)$ and $D(\theta)$ are both very small, but of a more similar relative magnitude. Actual changes in E and D (in mm/day) are miniscule in these regions, as seen in main text Figure 2d.